British Journal of Pharmacology (2004) 143, 19–26
www.nature.com/bjp

Differential agonist sensitivity of glycine receptor α2 subunit splice variants

[1]Paul S. Miller, [2]Robert J. Harvey & *,[1]Trevor G. Smart

[1]Department of Pharmacology, University College London, Gower Street, London WC1E 6BT and [2]Department of Pharmacology, The School of Pharmacy, 29–39 Brunswick Square, London WC1N 1AX

1 The glycine receptor (GlyR) α2A and α2B splice variants differ by a dual, adjacent amino acid substitution from $\alpha2A^{V58,T59}$ to $\alpha2B^{I58,A59}$ in the N-terminal extracellular domain.

2 Comparing the effects of the GlyR agonists, glycine, β-alanine and taurine, on the GlyR α2 isoforms, revealed a significant increase in potency for all three agonists at the α2B variant.

3 The sensitivities of the splice variants to the competitive antagonist, strychnine, and to the biphasic modulator Zn^{2+}, were comparable. In contrast, the allosteric inhibitor picrotoxin was more potent on GlyR α2A compared to GlyR α2B receptors.

4 Coexpression of α2A or α2B subunits with the GlyR β subunit revealed that the higher agonist potencies observed with the α2B homomer were retained for the α2Bβ heteromer.

5 The identical sensitivity to strychnine combined with a reduction in the maximum current induced by the partial agonist taurine at the GlyR α2A homomer, suggested that the changed sensitivity to agonists is in accordance with a modulation of agonist efficacy rather than agonist affinity.

6 An effect on agonist efficacy was also supported by using a structural model of the GlyR, localising the region of splice variation to the proposed docking region between GlyR loop 2 and the TM2-3 loop, an area associated with channel activation.

7 The existence of a *spasmodic* mouse phenotype linked to a GlyR $\alpha1^{A52S}$ mutation, the equivalent position to the source of the α2 splice variation, raises the possibility that the GlyR α2 splice variants may be responsible for distinct roles in neuronal function.
British Journal of Pharmacology (2004) **143,** 19–26. doi:10.1038/sj.bjp.0705875

Keywords: Glycine receptor; splice variants; molecular modelling; picrotoxin; strychnine; agonist efficacy; taurine; β-alanine; α2 subunit

Abbreviations: GlyR, glycine receptor; PTX, picrotoxin

Introduction

Glycine receptors (GlyRs) are the predominant type of inhibitory synaptic receptor present in the vertebrate hindbrain and spinal cord (Aprison & Daly, 1978). Together with $GABA_A$, serotonin ($5HT_3$) and nicotinic acetylcholine (ACh) receptors, GlyRs constitute the Cys-loop-based ligand-gated ion channel superfamily (Grenningloh *et al*., 1987). A pentameric quaternary structure has been proposed for the GlyR (Langosch *et al*., 1988), with variation in the receptor subunit composition resulting from the inclusion of different combinations of individual subunits into the final pentamer.

Molecular cloning studies of the GlyR have identified four subtypes of ligand-binding α subunit (α1–4) and a single subtype of the structural β subunit (Harvey *et al*., 2000). These α variants can be distinguished by their temporal and spatial expression patterns in the nervous system. For example, GlyR α2 and GlyR α4 are expressed throughout late embryonic stages with a developmental switch occurring during early postnatal maturation to favour expression of GlyR α1 and GlyR α3 isoforms (Takahashi *et al*., 1992; Singer *et al*., 1998; Harvey *et al*., 2000). In terms of spatial distribution, GlyR α1 and GlyR α2 have a more widespread pattern of expression (Kuhse *et al*., 1991; Malosio *et al*., 1991b) compared to GlyR α3 and GlyR α4 (Nikolic *et al*., 1998; Harvey *et al*., 2000).

The GlyR α subunits are afforded additional variation *via* alternative splicing of the primary gene transcripts (Harvey *et al*., 2000). For example, the α1 subunit exists in two isoforms: α1 and $\alpha1^{INS}$. The latter contains an extra consensus sequence for possible protein kinase phosphorylation in the form of an eight amino acid insertion within the large intracellular region between transmembrane domains (TM) 3–4 (Malosio *et al*., 1991a). In addition, GlyR α3 subunit transcripts also show alternative splicing in this region, producing two isoforms (α3S and α3L), which differ by 15 amino acids (Nikolic *et al*., 1998). By contrast, the GlyR α2A and GlyR α2B splice variants differ in the extracellular N-terminal domain by a dual amino acid substitution at positions 58 and 59 in the mature proteins (Kuhse *et al*., 1991). To date, this GlyR $\alpha2A^{V58,T59}$ to GlyR $\alpha2B^{I58,A59}$ substitution has not been attributed with any functional significance. However, in this context, it is noteworthy that the mouse line, *spasmodic*, harbours a GlyR $\alpha1^{A52S}$ mutation at the equivalent position to the GlyR $\alpha2A^{T59}$ and GlyR $\alpha2B^{A59}$ substitution. This mutation

*Author for correspondence; E-mail: t.smart@ucl.ac.uk
Advance online publication: 9 August 2004

in the α1 subunit results in a reduced agonist potency for glycine, taurine and β-alanine (Ryan *et al*., 1994; Saul *et al*., 1994).

With regard to these observations, we cloned and then characterised the GlyR α2A and GlyR α2B splice variants to assess their responses to glycine receptor agonists, and to modulators that could be of relevance physiologically. Our results indicate that positions 58 and 59 in the GlyR α2 subunit can determine the potencies for glycine, taurine and β-alanine. Studies using the partial agonist taurine, the competitive antagonist strychnine, and a structural model compiled for the GlyR α2 subunit, further suggest that the modulation of agonist potency by the amino acids occupying positions 58 and 59 do so, most likely, by affecting agonist efficacy rather than affinity.

Methods

Molecular biology

The following wild-type (wt) human GlyR expression constructs were used: GlyR α1L (Harvey *et al*., 1999), GlyR α2A, GlyR α2B and GlyR β (Handford *et al*., 1996). Human GlyR α2A and α2B cDNAs were amplified from embryonic whole-brain first-strand cDNA and cloned into the vector pCIS2 (Harvey *et al*., 1999) using the 'Seamless' cloning kit (Stratagene) using the primers pCIS1 5′-cggctcttctcacttgtttattg cagctta-3′, pCIS2 5′-aaactcttcatggcggccgcggacctcgag-3′, HA25 5′-caactcttcaccaggaatgaaccggcagctagtgaac-3′ and HA23 5′-cccctcttctgtggggcacatctatttcttgtggaca-3′ and PCR conditions as recommended by the manufacturer. Site-directed mutagenesis was performed using the Quikchange kit (Stratagene). All plasmid constructs and mutants were verified by DNA sequencing using the BigDye terminator cycle sequencing kit (Perkin-Elmer/ABI) and an Applied Biosystems 310 automated DNA sequencer prior to testing.

Cell culture and transfection

HEK cells (ATCC CRL1573) were grown in Dulbecco's modified Eagle's medium (DMEM) supplemented with 10% foetal calf serum (FCS), 2 mM glutamine, 100 U ml^{-1} penicillin G and 100 μg ml^{-1} streptomycin, incubated at 37°C in 95% air–5% CO_2 (Smart *et al*., 1991). Cells were transfected by electroporation at 400 V, infinite resistance, 125 μF using a Biorad Gene Electropulser II. Plasmids containing GlyR cDNA clones were cotransfected 1 : 1 with a reporter plasmid expressing the S65T mutant jellyfish green fluorescent protein (GFP). To ensure coexpression of GlyR αβ heteromers, the GlyR β subunit expression construct was mixed with GlyR α subunit plasmids at a ratio of 20 : 1. Cells were plated to achieve 20% confluence on poly-L-lysine (100 μg ml^{-1})-coated coverslips and then used for electrophysiology the next day.

Solutions

The internal patch pipette solution contained (mM): 140 KCl, 2 $MgCl_2$, 1 $CaCl_2$, 10 HEPES, 11 EGTA, and 2 ATP, pH 7.11 (≈300 mOsm). The external Krebs solution consisted of (mM): 140 NaCl, 4.7 KCl, 1.2 $MgCl_2$, 2.5 $CaCl_2$, 10 HEPES, and 11 D-Glucose, pH 7.4 (≈300 mOsm).

Electrophysiology

An Axopatch 200B amplifier (Axon instruments) was used to record whole-cell currents from single HEK cells using the patch-clamp technique. A holding potential of −40 mV was applied to HEK cells exhibiting resting potentials between −10 and −40 mV. Cells were visualised with an inverted differential interference contrast Nikon microscope with a fluorescence attachment to identify GFP transfected cells. A glass Y-tube was used to rapidly apply drugs and Krebs solutions (exchange rate approximately 50–100 ms) to the recorded cells. Patch electrodes were pulled using a Narashige PC-10 puller with resistances, after polishing, of 4–5 MΩ. All recordings were performed in constantly perfusing Krebs solution (5 ml min^{-1}) at room temperature (20–22°C).

Data acquisition and analysis

All current signals were filtered using a high-pass Bessel filter set to 3 kHz (−36 dB per octave). Data were recorded in 20-s acquisition periods directly to a Pentium IV, 1.8 GHz computer into Clampex 8.0 *via* a Digidata 1322A (Axon instruments) interface sampling at 200 μs intervals. Membrane current responses were assessed by applying two separate applications of an agonist. Before and after these applications, an EC_{50} concentration of the agonist (designated as a control) was applied to assess for any run-up or run-down in response amplitude during the experiments. If the two control response amplitudes varied by more than 15%, the experiment was discarded. The EC_{50}s for taurine and β-alanine, were determined from concentration–response curves normalised with respect to the maximum current activated by glycine (1 mM) measured in the same cells. For the experiments with picrotoxin, strychnine or Zn^{2+}, the HEK cell was preincubated with different concentrations of the inhibitor for 15 s to ensure full equilibration before applying EC_{50} concentrations of glycine in the presence of the antagonist. These agonist responses in the presence of the inhibitor were normalised by linear interpolation between the two surrounding control agonist response amplitudes determined in the absence of the inhibitor. The digitised currents were analysed offline using Axoscope 8.2. The biphasic curves, describing the Zn^{2+} concentration–response data, were generated using a nonlinear least-squares routine according to the following modified Hill equation, which assumes Zn^{2+} binds to two distinct sites, one producing potentiation and the other inhibition of the glycine-activated membrane current (Harvey *et al*., 1999):

$$I = I_{\min} + (I_{\max} - I_{\min})\,([1/(1 + (EC_{50}/B)^{n_H})] - [1/(1 + (IC_{50}/B)^{m_H})])$$

where I and $I_{\max}$ represent the modulated peak glycine-activated currents by a concentration of Zn^{2+}, B, and by a saturating concentration of Zn^{2+} respectively. $I_{\min}$ represents the control glycine current in the absence of the modulator and was set to 100%. EC_{50} and IC_{50} define the Zn^{2+} concentrations producing a half-maximal potentiating effect and a 50% inhibition of the maximally potentiated current, respectively. Both n_H and m_H represent the respective Hill coefficients.

The agonist concentration–response curves were fitted with the Hill equation,

$$I/I_{\max} = [(1/1 + (EC_{50}/A)^{n})]$$

where EC_{50} represents the concentration of agonist (A) inducing 50% of the maximal current evoked by a saturating concentration of agonist and n is the Hill coefficient. For the concentration-inhibition curves, the following equation was used:

$$I/I_{max} = 1 - [(1/1 + (IC_{50}/A)^n)]$$

where IC_{50} represents the concentration of the inhibitor causing a 50% reduction in the agonist-activated response. Any statistical comparisons were carried out using an unpaired t-test.

Modelling

The mature N-terminal extracellular domain (ECD) of the human GlyR α2 subunit, was modelled on the crystal structure of the acetylcholine-binding protein (AChBP; Brejc *et al*., 2001) using SwissProt DeepView in accordance with a ClustalW protein alignment. The GlyR transmembrane domains, TM1-3, and separately TM4, were aligned and modelled on the atomic structure of the Torpedo nicotinic acetylcholine receptor (nAChR) chain A imported into SwissProt DeepView (Miyazawa *et al*., 2003). The GlyR ECD and TMs were then empirically docked to ensure that: the C-terminus of the ECD linked with the N-terminus of TM1; the TM2-3 loop was closely apposed to the base of the N-terminal Cys loop; and that the N-terminal domains did not sterically hinder each other when assembled in a pentameric complex.

Results

Agonist sensitivity of GlyR α2A and GlyR α2B

Expression constructs for the human GlyR α2A and α2B isoforms were generated by cloning full-length α2 subunit cDNAs from embryonic whole-brain first-strand cDNA into the expression vector pCIS2. The sequences of the human α2A and α2B variants have been deposited in the GenBank database under the Accession Numbers AY437083 and AY437084. The protein sequences for the α2 isoforms over the region of variance, in comparison with GlyR α1, α3 and α4 subunits, are shown in Figure 1a. Whole-cell recordings from transfected HEK cells expressing either GlyR α2A or GlyR α2B were used to assess the relative sensitivities to the three agonists, glycine, taurine and β-alanine (Figure 1e, f), by comparing the agonist concentration–response curves on each receptor isoform (Figure 1b–d). These revealed that the three agonist potencies were significantly different between the GlyR α2 splice-variants with the EC_{50}s determined on the GlyR α2B

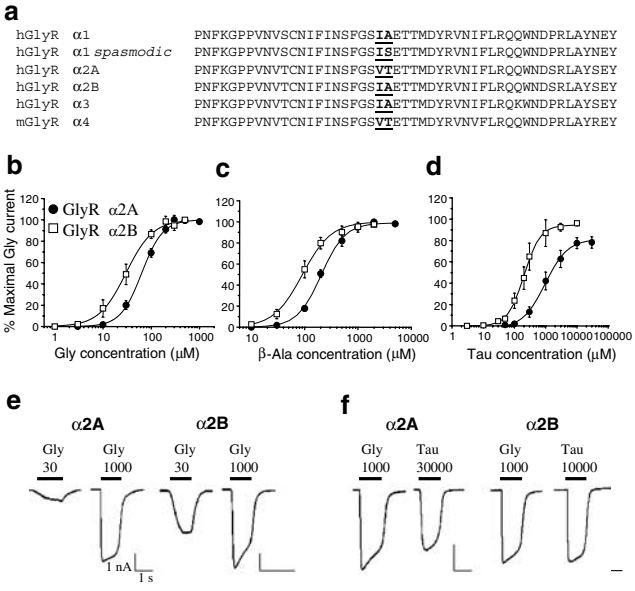

Figure 1 Differential agonist sensitivities of the GlyR α2A and GlyR α2B isoforms expressed in transfected HEK cells: (a) protein sequence alignment of GlyR α subunits highlighting in bold the region of splice variation between α2A and α2B. 'h' signifies human and 'm' murine sequences. (b–d) Agonist concentration–response curves for the activation of GlyR splice variants α2A and α2B by glycine (b), β-alanine (c) and taurine (d). The dose–response data for glycine, β-alanine and taurine are all normalised to the response activated by 1 mM glycine (= 100 %) within the same cell. (e) Selected glycine (Gly)-activated currents showing differential agonist potency for GlyR α2A and GlyR α2B for 30 μM Gly compared to a saturating concentration of 1000 μM Gly. (f) Glycine and taurine (Tau)-activated currents showing the maximal current activated by 10–30 mM taurine at GlyR α2A and GlyR α2B, in comparison to a saturating concentration of glycine (1 mM). Note that the increased osmolarity due to 30 mM taurine did not affect the current amplitude as 30 mM taurine applied to untransfected cells did not evoke any current (data not shown). The calibration bars represent 1 nA and 1 s. In this and succeeding figures the points represent the mean ± s.e., $n = 4$–13 cells.

Table 1 Ligand potencies determined on wild-type and mutant GlyRs

Subunit	*Glycine*			*Taurine*		β-*Alanine*	
	EC_{50} (μM)	*Hill slope*	I_{max} (nA)	EC_{50} (μM)	*Hill slope*	EC_{50} (μM)	*Hill slope*
GlyRα2A	66 ± 7[a]	1.9 ± 0.2	4.3 ± 0.2	1280 ± 350[a]	1.3 ± 0.1[b]	210 ± 24[a]	1.9 ± 0.2
GlyRα2Aβ	65 ± 8[a]	2.4 ± 0.3	4.0 ± 0.2	1460 ± 350[a]	1.1 ± 0.1[b]	181 ± 23[a]	1.8 ± 0.1
GlyRα2B	34 ± 6	1.9 ± 0.2	3.8 ± 0.2	310 ± 140	1.8 ± 0.2	92 ± 19	1.7 ± 0.2
GlyRα2Bβ	27 ± 2	2.5 ± 0.2	4.2 ± 0.5	320 ± 10	1.6 ± 0.1	90 ± 20	1.8 ± 0.1
GlyRα2B^{I58V}	28 ± 6	2.2 ± 0.3	5.2 ± 0.3	500 ± 100	1.4 ± 0.1		
GlyRα2B^{A59T}	65 ± 9[a]	2.6 ± 0.3	4.7 ± 0.8	830 ± 120[a]	1.4 ± 0.2		

The ligand EC_{50}s and Hill slopes were obtained from the Hill equation curve fits to the concentration–response data. I_{max} indicates the maximal-activated current by saturating concentrations of glycine (1 mM). All values are means ± s.e. with the number of determinations ranging from 4 to 13.
[a]EC_{50}s significantly higher than for the GlyR α2B counterpart using an unpaired t-test ($P < 0.05$).
[b]Taurine Hill slopes significantly lower than their glycine Hill slope counterparts ($P < 0.05$).

being 2–4-fold lower than those obtained with α2A ($P<0.05$; Table 1). Taurine exhibited the clearest difference in potency with the EC_{50} increasing from $305\pm138\,\mu$M for GlyR α2B to $1290\pm305\,\mu$M for GlyR α2A (mean±s.e.; $n=5$ and 6, respectively; $P<0.05$). Additionally, taurine was reduced from a virtual full agonist at GlyR α2B (maximum response compared to glycine of $97\pm1.8\%$) to a partial agonist at GlyR α2A ($84\pm3.9\%$; $P<0.05$). The Hill slopes for the glycine and β-alanine concentration–response curves were comparable between the two receptor splice variants, varying from 1.7 to 2.6, but this was reduced for taurine to between 1.1 and 1.8 (Table 1), consistent with previous observations (Schmieden *et al*., 1992).

Effects of the modulators, picrotoxin, strychnine and Zn^{2+}, on the splice variant GlyR α2 subunits

The GlyR α2A and GlyR α2B receptor isoforms were characterised further by measuring the potencies of three prominent GlyR inhibitors, picrotoxin (PTX), strychnine and Zn^{2+} (Figure 2a–c). The two splice variants were differentially sensitive by approximately five-fold to picrotoxin with the IC_{50} increasing from $0.79\pm0.1\,\mu$M for GlyR α2A to $4.1\pm1.3\,\mu$M for GlyR α2B ($n=7$; $P<0.05$). For strychnine and Zn^{2+}, the IC_{50}s were comparable between the two GlyR α2 isoforms (GlyR α2A IC_{50}s: strychnine 36 ± 10 nM, Zn^{2+} $512\pm75\,\mu$M; compared to GlyR α2B IC_{50}s: strychnine, 27 ± 1 nM, Zn^{2+} $454\pm49\,\mu$M; $n=4$–9; $P>0.05$). Moreover, the biphasic modulation of glycine-activated currents that typifies Zn^{2+} modulation of GlyRs was also present for the GlyR α2 splice variants. The sensitivity to potentiating Zn^{2+} and the size of the potentiation of currents activated by EC_{50} concentrations of glycine remained unaffected by the differences in structure between GlyR α2A and GlyR α2B (Figure 2c).

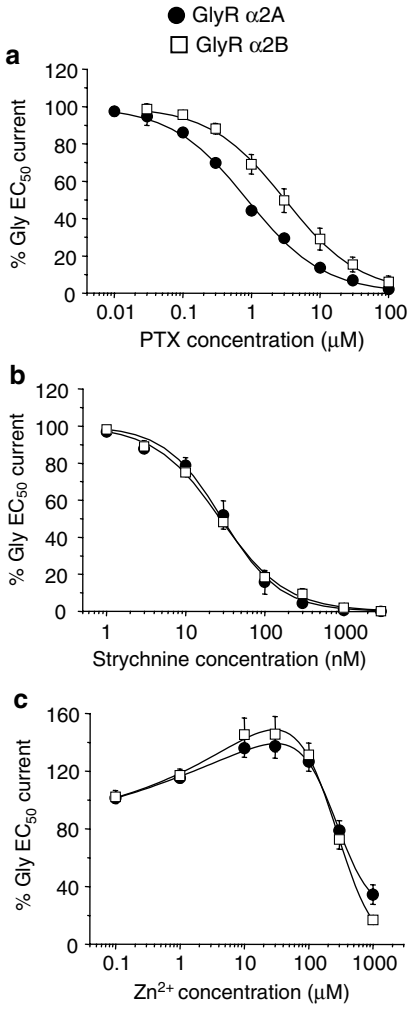

Figure 2 Comparison of glycine receptor antagonist potencies between GlyR α2A and GlyR α2B splice variants: inhibitory concentration–response curves were determined for the EC_{50} glycine-activated current recorded from GlyR α2A- and GlyR α2B-expressing HEK cells. (a) Picrotoxin (PTX) shows a five-fold increased potency at the GlyR α2A compared to the GlyR α2B isoform ($P<0.05$). (b) Strychnine sensitivity displays identical profiles at either GlyR α2 isoform. (c) The biphasic profile of Zn^{2+} on GlyR α2A and GlyR α2B is indistinguishable for both the potentiating and inhibitory modulatory phases. Data from $n=4$–8 cells.

Role of individual amino acids in the splice region on agonist and antagonist sensitivities of GlyRs

A previously identified mutation GlyR $\alpha1^{A52S}$, that underlies the *spasmodic* mouse phenotype and is responsible for a reduced agonist potency (Ryan *et al*., 1994; Saul *et al*., 1994), is located at the equivalent residue to the GlyR $\alpha2B^{A59}$ to GlyR $\alpha2A^{T59}$ splice variation. We therefore investigated the relative effect of each of the two amino acid differences between the α2A and α2B splice variants by exchanging them individually. The GlyR $\alpha2B^{I58V}$ and GlyR $\alpha2B^{A59T}$ mutants were compared for glycine, taurine and PTX sensitivity, which were already known to differ in potency between the α2 isoforms (Figure 3a–c). For glycine and PTX, the different potencies caused by the splice variation are abolished when the GlyR $\alpha2B^{A59T}$ mutation is compared to wild-type GlyR α2A (Figure 3a, c); however, the GlyR $\alpha2B^{I58V}$ mutant exhibited sensitivities to glycine and PTX that directly overlayed those of the wild-type GlyR α2B. With regard to taurine, individual substitution of either GlyR α2B I58 or A59 to the GlyR α2A equivalents caused a partial but incomplete change in the EC_{50} towards GlyR α2A levels of sensitivity (Figure 3b). This reached significance for $\alpha2B^{A59T}$, which had a higher EC_{50} compared to its α2B wild-type counterpart ($P<0.05$; Table 1).

Sensitivity to ligands of heteromeric GlyRs incorporating the α2 subunit splice variants

To examine the relative potencies of glycine, taurine and PTX for GlyR α2A and GlyR α2B in a more physiological context, the α subunits were coexpressed in HEK cells with the GlyR β subunit (Figure 4). The concentration–response curves, constructed for each agonist with either GlyR α2Aβ or GlyR α2Bβ, retained the differences first observed with the α2 homomeric splice variants. Thus, the agonist EC_{50}s determined on GlyR α2Bβ demonstrated an approximate two- and four-fold reduction for glycine (Figure 4a) and taurine (Figure 4b) respectively, when compared to the agonist EC_{50} determinations on the GlyR α2Aβ. The increased GlyR α2Aβ agonist EC_{50}s reached significance for all three agonists tested, glycine,

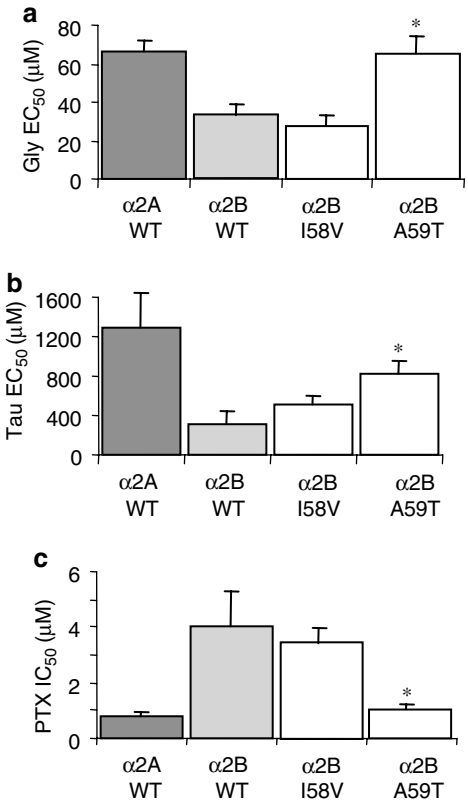

Figure 3 Importance of individual amino acids within the α2 subunit splice variation on ligand potency: the top, middle and lower panels depict bargraphs of the EC_{50}s for glycine (a) and taurine (b), and the PTX IC_{50}, determined using glycine (EC_{50})-activated currents (c), respectively. These potencies were determined on wild-type (WT) GlyR α2A and GlyR α2B isoforms, and on the single amino acid mutants, GlyR $\alpha2B^{I58V}$ and GlyR $\alpha2B^{A59T}$. All bars represent means ± s.e. from $n = 4$–13 cells. Potencies determined on GlyR $\alpha2B^{A59T}$ were significantly different (*) from wild-type GlyR α2B for glycine, taurine and PTX ($P < 0.05$); while GlyR $\alpha2B^{I58V}$ did not show any significant difference at the 5% level for all three ligands.

taurine and β-alanine ($P < 0.05$; Table 1). In complete contrast, the differential potency of PTX was abolished by coexpression of either the GlyR α2A or α2B subunit with the β subunit, producing comparable IC_{50}s (α2Aβ, 13.2 ± 1.4 μM; α2Bβ, 15.8 ± 4.2 μM, $n = 4$; $P > 0.05$; Figure 4c).

The sensitivity to PTX is known to be significantly reduced upon coexpression of GlyR α and β subunits (Pribilla *et al*., 1992; Handford *et al*., 1996). The coincidence of the PTX inhibition response curves for the two heteromers in our study is unlikely to be due to less efficient incorporation of the β subunit into the α2Bβ heteromer, because the IC_{50} does shift from that observed with the α2B homomer and a biphasic inhibition curve, indicative of a mixture of α2B homomers and α2Bβ heteromeric receptors, is not evident. Moreover, any reduced efficiency in coassembly would have to be quite significant as β subunits were transfected at markedly saturating cDNA ratios of 20β : 1α to ensure full incorporation of the β subunit. Thus, it would appear that for the receptor's sensitivity to PTX, the β subunit plays a dominant role overriding the effect of the splice variation in the α2 subunit.

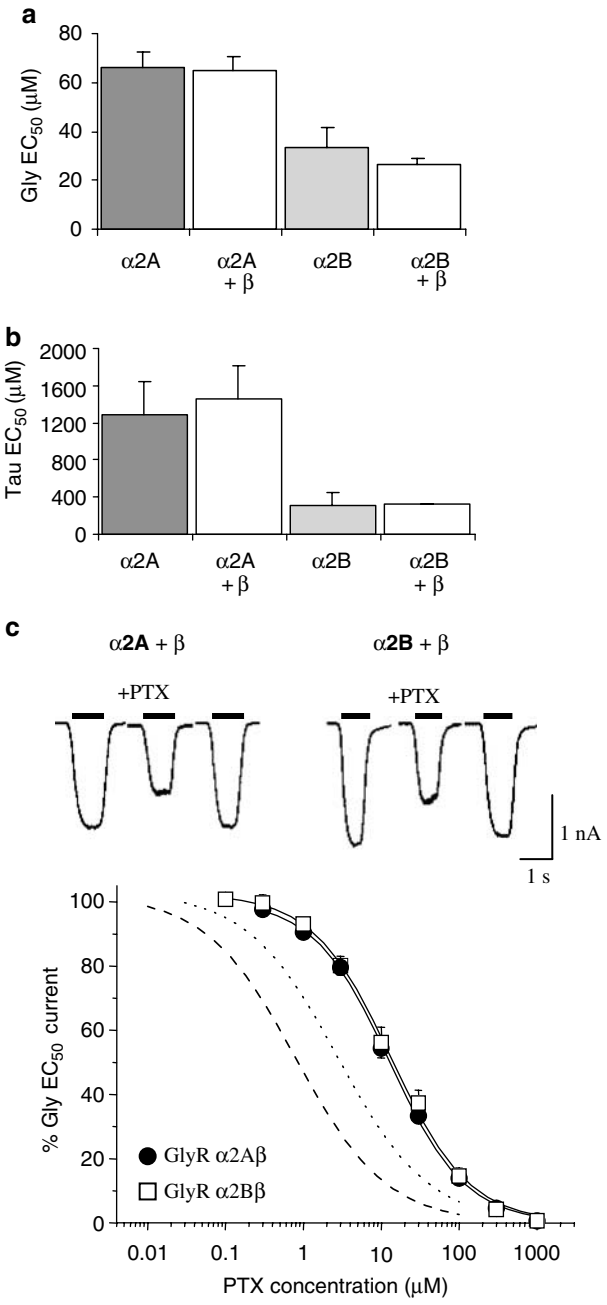

Figure 4 Influence of the β subunit on the α2 splice variant heteromeric GlyRs: (a, b) bargraphs of glycine and taurine EC_{50}s, measured for GlyR α2A and GlyR α2B homomers and when coexpressed with the β subunit ($n = 4$–13 cells). Data for the wild-type homomeric receptors are taken from Figure 3 for comparison. (c) Upper panel, typical membrane currents activated by EC_{50} concentrations of glycine (solid lines) before and after recovery from the coapplication of 10 μM PTX. Lower panel, PTX concentration curves obtained from the inhibition of EC_{50} glycine-activated currents for GlyR α2A and α2B separately coexpressed with the GlyR β subunit ($n = 4$ cells). For comparison, the curve fits for the PTX inhibition of glycine responses recorded from homomeric GlyR α2A (dashed line) and GlyR α2B (dotted line) are shown (data taken from Figure 2a).

Discussion

This study demonstrates that the GlyR α2B has a significantly higher sensitivity to the agonists, glycine, β-alanine and

taurine, compared to the GlyR α2A isoform and that this functional difference can be accounted for by a region involving just two residues in the N-terminal extracellular domain, *vis* the $\alpha2A^{V58,T59}$ to $\alpha2B^{I58,A59}$ substitution. Although another GlyR α2 isoform has recently been identified, α2N, the mRNA for this subunit lacks the GlyR α2 exon 3 coding region, which includes the α2A and α2B source of splice variation (Kumar *et al*., 2002). Since a corresponding α2N protein would suffer a significant truncation during synthesis that is capable of perturbing function and as yet, has not been isolated, it was not considered for comparison in this study.

Exchanging two amino acids in GlyR α2 subunits affects agonist sensitivity

The α2A and α2B splice variant amino acids reduced agonist potency in a similar manner and by a similar extent, approximately a two-fold reduction, to that reported for a GlyR $\alpha1^{A52S}$ mutation. The fact that the reduction in agonist sensitivities could be considered modest in the *spasmodic* mouse suggests that for GlyR α1 subunits, these subtle changes in receptor function can actually be responsible for quite substantial perturbations to the animal phenotype. If these phenotypic implications can also be extended to the GlyR α2 splice variants, it further suggests that the subtle difference in agonist sensitivities may be sufficient to optimise each of the GlyR α2 isoforms for specific physiological roles. This concept may have relevance for a recent study that reported that the homomeric GlyR α2A subtype only supports a slow rate of activation following glycine binding. Thus, this receptor was considered unlikely to be activated by the expected release profile of glycine and its likely concentration in the synaptic cleft (Mangin *et al*., 2003). In the case of GlyR α2B, the increase in sensitivity to glycine may make this variant a more likely candidate to respond to the synaptic release of agonist, especially if the activation kinetics are also faster. The whole-cell currents activated by glycine in the present study did not seem to be overtly different for the rate of activation between α2A and α2B; however, this requires ultrafast perfusion to a macropatch-containing glycine receptors for verification.

Partial agonists and the GlyR α2 splice variants

The reduction in the maximal current activated by saturating concentrations of taurine on GlyR α2A compared to GlyR α2B suggested that the $\alpha2A^{V58,T59}$ to $\alpha2B^{I58,A59}$ substitution might, instead of reducing agonist affinity, be reducing agonist efficacy (E) instead. If only agonist affinity was compromised by the residue exchange then a shift in the EC_{50} without a reduction in the maximal current would be expected. For both glycine and *β*-alanine, the maximal responses did not appear to vary between the GlyR α2 subunit splice variants. Although this may suggest that the amino acid splice variant is differentially affecting agonist activation, it may also be in accordance with a mechanism based on agonist efficacies, since these will determine, to some extent, the degree of maximum response depression. For example, for high-efficacy agonists, a modest shift in potency, as described here, would be expected to result in a simple parallel shift in the concentration–response curves (Colquhoun, 1998).

GlyR topology: the region of splice variation

The generation of a GlyR topological model based on the AChBP (see Methods, Figure 5) positions the GlyR $\alpha2A^{V58,T59}$ to GlyR $\alpha2B^{I58,A59}$ substitution close to the base of the N-terminal extracellular domain. In comparison, the putative PTX-binding site (Pribilla *et al*., 1992) is thought to be located within the ion channel lining (residues A261–R278), directly below the region of splice variation. The proximity between these two domains may be the reason why the homomeric GlyR α2A and α2B splice variants differentially affect the antagonist action of PTX. Indeed, PTX can affect ion channel gating (Smart & Constanti, 1986; Newland & Cull-Candy, 1992) and if these GlyR α2 subunit splice site residues are potentially close to, or actually part of, a pathway that links the agonist-binding site to channel activation, it would not be

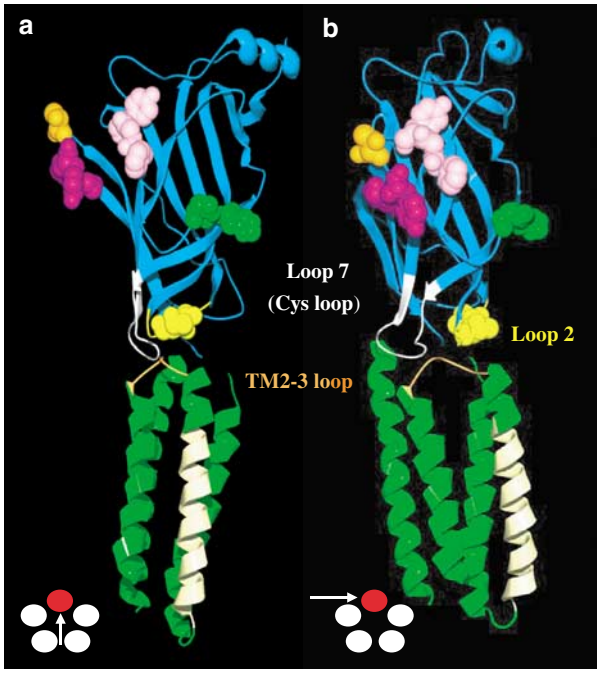

Figure 5 Topological model of the GlyR N-terminal domain linked to the GlyR transmembrane domains: the views are taken from an elevation of the internal face of the receptor ((a) see pictogram of the GlyR in plan view with the subunits represented as white and red circles. The line of view is represented by the white arrows) and from a side elevation of the subunit (b). The GlyR extracellular N-terminal domain is depicted as blue ribbons with the TM1–4 displayed in green and cream ribbons and the TM2–3 loop shown as orange. From this study and others, the N-terminal residues that are important for ligand potency are space-filled, while the putative PTX-binding site/domain (Pribilla *et al*., 1992) is highlighted in the TM2 region as a pale cream ribbon (GlyR α2, residues A261–R278). Purple residues (GlyR α2 K207, Y209) and pink residues (GlyR α2 F166–Y168) are important for glycine and strychnine potency, the orange residue (GlyR α2 T211) selectively affects only the potency of glycine (Vandenberg *et al*., 1992a, b). The green residues, N114 and H116, modulate Zn^{2+} inhibition (Harvey *et al*., 1999). The white ribbon delineates the Cys loop (GlyR α2, residues C145–159), which is considered to be important for agonist gating in ligand-gated ion channels (Kash *et al*., 2003; Miyazawa *et al*., 2003). The two yellow residues (GlyR α2 V58, T59) represent the location of the splice variation between GlyR α2A and GlyR α2B. Note the physical proximity of these residues to the Cys loop region and the TM2–3 loop.

surprising for them to affect concurrently PTX inhibition and agonist potency. However, the selective role of the β subunit in abolishing the effect of the splice variation on PTX inhibition but not on agonist potency is intriguing. When the two β subunits are present in the receptor complex (assuming the consensus $\alpha_3\beta_2$ stoichiometry of a heteromeric receptor), it may indicate that the transduction pathway is only altered from the PTX-binding site, since the β subunits introduce a common structural component, and this appears sufficient to recover comparable PTX sensitivity for the GlyR α2Aβ and α2Bβ heteromers, even though they retain their distinctive agonist sensitivities. Such a result is incompatible with there being only one linear transduction pathway involving both PTX- and agonist-binding sites.

In contrast to PTX, the proposed strychnine (Vandenberg *et al*., 1992a) and Zn^{2+} inhibitory binding sites (Harvey *et al*., 1999), together with the region implicated in agonist binding (Vandenberg *et al*., 1992b; Schmieden *et al*., 1993), are all predicted to be located further away from the membrane interface, distal to the variation in the GlyR α2 structure introduced by RNA alternative splicing. Thus, any communication between these 'competitive-type' antagonists and the predicted agonist-binding site, whether direct in the probable case of strychnine, or indirect but still apparently competitive (Laube *et al*., 1995) in the case of the inhibitory Zn^{2+} site, may not need to pass close to or *via* the region of splice variation. Under these circumstances, the antagonist potencies would be expected not to differ between the splice variants. Interestingly though, Zn^{2+} has been postulated to affect glycine-activated channel gating (Laube *et al*., 2000), but since Zn^{2+} inhibition is unaffected by the splice site variation, presumably there must be another transduction pathway that can affect GlyR ion channel gating avoiding the splice site, one that is not used by agonist-activated gating.

Further support for the spice variation exerting an efficacy-mediated effect rather than a direct perturbation of the agonist-binding site can be gained by considering the strychnine-binding site. Given that strychnine is thought to require some overlapping residues with the agonist recognition site to act as a competitive antagonist on the glycine receptor (Vandenberg *et al*., 1992a), this suggests that at least part of the agonist-binding region is not disrupted by the N-terminal dual amino acid substitution in the α2 subunit. In the case of the topological model (Figure 5) this predicts that the site of the α2 splice variation is located immediately prior to loop 2 (according to the nomenclature of Brejc *et al*.) far from the proposed agonist and strychnine-binding region, but directly adjacent to the Cys-loop region (loop 7) of the receptor. This implies, spatially, that it is simpler for the $\alpha2A^{V58,T59}$ to $\alpha2B^{I58,A59}$ substitution to distort residues at the immediate apex of loop 2, an area previously suggested to be capable, in the homologous nAChR, of docking directly with the M2 helix, *via* an nAChR α1 subunit valine residue (V44; Miyazawa *et al*., 2003). Additionally, this splice variant could also affect the neighbouring Cys-loop, a region that along with loop 2 was previously implicated as being important for the gating of the ligand-gated ion channel superfamily (Kash *et al*., 2003). However, it should be noted that these results do not discount a combination of effects on agonist binding and efficacy caused by the splice variant residues.

Taken together, these data represent the first comparative characterisation of the GlyR α2A and GlyR α2B splice variants. A clear and distinct difference in sensitivity is apparent between the two α2 subunit isoforms to the physiologically relevant agonists, glycine and taurine. While the agonist potency shifts appear relatively small, the existence of a *spasmodic* mouse, GlyR $\alpha1^{A52S}$ mutation, at the same location as the source of GlyR α2 splice variation, suggests these subtle molecular differences may be sufficient to imbue the GlyR α2A and α2B with distinct and relevant functional roles.

This work was supported by the MRC and the Wellcome Trust. Paul Miller is in receipt of a Wellcome Trust 4-year PhD postgraduate studentship. We also thank Alastair Hosie for help with the GlyR α2 structural modelling and Peter Schofield for providing the human glycine receptor β subunit expression construct.

References

APRISON, M.H. & DALY, E.C. (1978). Biochemical aspects of transmission of inhibitory synapses. *Adv. Neurochem,* **3,** 203–294.

BREJC, K., VAN DIJK, W.J., KLAASSEN, R.V., SCHUURMANS, M., VAN DER, O.J., SMIT, A.B. & SIXMA, T.K. (2001). Crystal structure of an ACh-binding protein reveals the ligand-binding domain of nicotinic receptors. *Nature,* **411,** 269–276.

COLQUHOUN, D. (1998). Binding, gating, affinity and efficacy: the interpretation of structure–activity relationships for agonists and of the effects of mutating receptors. *Br. J. Pharmacol.,* **125,** 924–947.

GRENNINGLOH, G., GUNDELFINGER, E., SCHMITT, B., BETZ, H., DARLISON, M.G., BARNARD, E.A., SCHOFIELD, P.R. & SEEBURG, P.H. (1987). Glycine vs GABA receptors. *Nature,* **330,** 25–26.

HANDFORD, C.A., LYNCH, J.W., BAKER, E., WEBB, G.C., FORD, J.H., SUTHERLAND, G.R. & SCHOFIELD, P.R. (1996). The human glycine receptor beta subunit: primary structure, functional characterisation and chromosomal localisation of the human and murine genes. *Brain Res. Mol. Brain Res.,* **35,** 211–219.

HARVEY, R.J., SCHMIEDEN, V., VON HOLST, A., LAUBE, B., ROHRER, H. & BETZ, H. (2000). Glycine receptors containing the alpha4 subunit in the embryonic sympathetic nervous system, spinal cord and male genital ridge. *Eur. J. Neurosci.,* **12,** 994–1001.

HARVEY, R.J., THOMAS, P., JAMES, C.H., WILDERSPIN, A. & SMART, T.G. (1999). Identification of an inhibitory Zn^{2+} binding site on the human glycine receptor alpha1 subunit. *J. Physiol.,* **520,** 53–64.

KASH, T.L., JENKINS, A., KELLEY, J.C., TRUDELL, J.R. & HARRISON, N.L. (2003). Coupling of agonist binding to channel gating in the GABA(A) receptor. *Nature,* **421,** 272–275.

KUHSE, J., KURYATOV, A., MAULET, Y., MALOSIO, M.L., SCHMIEDEN, V. & BETZ, H. (1991). Alternative splicing generates two isoforms of the alpha 2 subunit of the inhibitory glycine receptor. *FEBS Lett.,* **283,** 73–77.

KUMAR, D.V., NIGHORN, A. & ST JOHN, P.A. (2002). Role of nova-1 in regulating alpha2N, a novel glycine receptor splice variant, in developing spinal cord neurons. *J. Neurobiol.,* **52,** 156–165.

LANGOSCH, D., THOMAS, L. & BETZ, H. (1988). Conserved quaternary structure of ligand-gated ion channels: the postsynaptic glycine receptor is a pentamer. *Proc. Natl. Acad. Sci. U.S.A.,* **85,** 7394–7398.

LAUBE, B., KUHSE, J. & BETZ, H. (2000). Kinetic and mutational analysis of Zn^{2+} modulation of recombinant human inhibitory glycine receptors. *J. Physiol.,* **522** (Part 2), 215–230.

LAUBE, B., KUHSE, J., RUNDSTROM, N., KIRSCH, J., SCHMIEDEN, V. & BETZ, H. (1995). Modulation by zinc ions of native rat and recombinant human inhibitory glycine receptors. *J. Physiol.,* **483** (Part 3), 613–619.

MALOSIO, M.L., GRENNINGLOH, G., KUHSE, J., SCHMIEDEN, V., SCHMITT, B., PRIOR, P. & BETZ, H. (1991a). Alternative splicing generates two variants of the alpha 1 subunit of the inhibitory glycine receptor. *J. Biol. Chem.,* **266,** 2048–2053.

MALOSIO, M.L., MARQUEZE-POUEY, B., KUHSE, J. & BETZ, H. (1991b). Widespread expression of glycine receptor subunit mRNAs in the adult and developing rat brain. *EMBO J.,* **10,** 2401–2409.

MANGIN, J.M., BALOUL, M., PRADO, D.C., ROGISTER, B., RIGO, J.M. & LEGENDRE, P. (2003). Kinetic properties of the alpha2 homo-oligomeric glycine receptor impairs a proper synaptic functioning. *J. Physiol.,* **553,** 369–386.

MIYAZAWA, A., FUJIYOSHI, Y. & UNWIN, N. (2003). Structure and gating mechanism of the acetylcholine receptor pore. *Nature,* **424,** 949–955.

NEWLAND, C.F. & CULL-CANDY, S.G. (1992). On the mechanism of action of picrotoxin on GABA receptor channels in dissociated sympathetic neurones of the rat. *J. Physiol.,* **447,** 191–213.

NIKOLIC, Z., LAUBE, B., WEBER, R.G., LICHTER, P., KIOSCHIS, P., POUSTKA, A., MULHARDT, C. & BECKER, C.M. (1998). The human glycine receptor subunit alpha3. Glra3 gene structure, chromosomal localization, and functional characterization of alternative transcripts. *J. Biol. Chem.,* **273,** 19708–19714.

PRIBILLA, I., TAKAGI, T., LANGOSCH, D., BORMANN, J. & BETZ, H. (1992). The atypical M2 segment of the beta subunit confers picrotoxinin resistance to inhibitory glycine receptor channels. *EMBO J.,* **11,** 4305–4311.

RYAN, S.G., BUCKWALTER, M.S., LYNCH, J.W., HANDFORD, C.A., SEGURA, L., SHIANG, R., WASMUTH, J.J., CAMPER, S.A., SCHOFIELD, P. & O'CONNELL, P. (1994). A missense mutation in the gene encoding the alpha 1 subunit of the inhibitory glycine receptor in the spasmodic mouse. *Nat. Genet.,* **7,** 131–135.

SAUL, B., SCHMIEDEN, V., KLING, C., MULHARDT, C., GASS, P., KUHSE, J. & BECKER, C.M. (1994). Point mutation of glycine receptor alpha 1 subunit in the spasmodic mouse affects agonist responses. *FEBS Lett.,* **350,** 71–76.

SCHMIEDEN, V., KUHSE, J. & BETZ, H. (1992). Agonist pharmacology of neonatal and adult glycine receptor alpha subunits: identification of amino acid residues involved in taurine activation. *EMBO J.,* **11,** 2025–2032.

SCHMIEDEN, V., KUHSE, J. & BETZ, H. (1993). Mutation of glycine receptor subunit creates beta-alanine receptor responsive to GABA. *Science,* **262,** 256–258.

SINGER, J.H., TALLEY, E.M., BAYLISS, D.A. & BERGER, A.J. (1998). Development of glycinergic synaptic transmission to rat brain stem motoneurons. *J. Neurophysiol.,* **80,** 2608–2620.

SMART, T.G. & CONSTANTI, A. (1986). Studies on the mechanism of action of picrotoxinin and other convulsants at the crustacean muscle GABA receptor. *Proc. R. Soc. Lond. B,* **227,** 191–216.

SMART, T.G., MOSS, S.J., XIE, X. & HUGANIR, R.L. (1991). $GABA_A$ receptors are differentially sensitive to zinc: dependence on subunit composition. *Br. J. Pharmacol.,* **103,** 1837–1839.

TAKAHASHI, T., MOMIYAMA, A., HIRAI, K., HISHINUMA, F. & AKAGI, H. (1992). Functional correlation of fetal and adult forms of glycine receptors with developmental changes in inhibitory synaptic receptor channels. *Neuron,* **9,** 1155–1161.

VANDENBERG, R.J., FRENCH, C.R., BARRY, P.H., SHINE, J. & SCHOFIELD, P.R. (1992a). Antagonism of ligand-gated ion channel receptors: two domains of the glycine receptor alpha subunit form the strychnine-binding site. *Proc. Natl. Acad. Sci. U.S.A.,* **89,** 1765–1769.

VANDENBERG, R.J., HANDFORD, C.A. & SCHOFIELD, P.R. (1992b). Distinct agonist- and antagonist-binding sites on the glycine receptor. *Neuron,* **9,** 491–496.

(Received March 5, 2004
Revised April 28, 2004
Accepted May 11, 2004)